

Supplementary Information

Environmental stress-induced bacterial lysis and extracellular DNA release contribute to *Campylobacter jejuni* biofilm formation

Jinsong Feng, Lina Ma, Jiatong Nie, Michael E. Konkel, Xiaonan Lu*

MATERIALS AND METHODS

Construction of C. jejuni F38011 ΔspoT and ΔrecA mutant strains

C. jejuni F38011 *spoT* deletion mutant was generated via homologous recombination and subsequent insertion of a kanamycin resistance cassette. The gene sequence of *spoT* in *C. jejuni* F38011 was identical to the gene sequence of *spoT* (*Cj1272c*) in *C. jejuni* 11168, which was confirmed by nucleotide BLAST. A 430-bp upstream cassette of the *spoT* gene was PCR-amplified using the primer pair of *spoT*-FF/*spoT*-FR. Similarly, a 476-bp downstream cassette of the *spoT* gene was PCR-amplified using the primer pair of *spoT*-RF/*spoT*-RR. The kanamycin resistance gene (Kan^R) was amplified using the primer pair *kan*-F/*kan*-R from the plasmid pUC18K2 (gift from Dr. Erin Gaynor at University of British Columbia). The vector pUC19 was digested with EcoRI and XbaI. All the aforementioned four fragments were purified using the Gel/PCR purification kit (Froggabio), followed by multiple fragment ligation using NEBuilder® HiFi DNA Assembly Cloning Kit (New England Biolabs® INC.). The pUC19-*spoT*::Kan^R disruption construction was naturally transformed into *C. jejuni* F38011, as *C. jejuni* is a naturally competent bacterium (1). Transformants were selected on MHB agar plates supplemented with kanamycin (50 µg/ml). The deletion of *spoT* gene and insertion of Kan^R was identified by PCR.

C. jejuni F38011 *recA* deletion mutant was generated via homologous recombination and

subsequent insertion of a chloramphenicol resistance cassette. The gene sequence of *recA* in *C. jejuni* F38011 was identical to the sequence of *recA* (*Cj1673c*) in *C. jejuni* 11168, which was confirmed by nucleotide BLAST. A 428-bp upstream cassette of *recA* gene was PCR-amplified using the primer pair of *recA*-FF/*recA*-FR. Similarly, a 626-bp downstream cassette of *recA* gene was PCR-amplified using the primer pairs of *recA*-RF/*recA*-RR. The chloramphenicol resistance gene (Cm^{R}) was amplified using the primer pair of *cm*-F/*cm*-R from the plasmid pRY111 (gift from Dr. Brett Finlay at University of British Columbia). The vector pUC19 was digested with EcoRI and XbaI. All the aforementioned four fragments were purified using the Gel/PCR purification kit (Froggabio), followed by the multiple fragment ligation using NEBuilder® HiFi DNA Assembly Cloning Kit (New England Biolabs® Inc.). The pUC19-*recA*:: Cm^{R} disruption construction was naturally transformed into *C. jejuni* F38011. Transformants were selected on MHB agar plates supplemented with chloramphenicol (8 $\mu\text{g/ml}$). The deletion of *recA* gene and insertion of Cm^{R} was identified by PCR. The primer used for mutant construction was listed in **Table S2**.

Construction of C. jejuni F38011 spoT and recA complementary strains

The complementary plasmid for *spoT* gene was derived from pRY111 vector (a gift from Dr. Konkel at Washington State University). The insertion fragment containing upstream (500 bp) and downstream (150 bp) regions of *spoT* gene was PCR-amplified using primer pairs of *spoT*-CF/*spoT*-CR. The amplicon containing *spoT* gene was ligated with EcoRI/XbaI-digested pRY111 using NEBuilder® HiFi DNA Assembly Cloning Kit (New England Biolabs® Inc.). The complementary plasmid pRY111-*spoT* was then transformed into the *C. jejuni* F38011 $\Delta\textit{spoT}$ mutant. Transformants were selected on MH agar supplemented with chloramphenicol (8 $\mu\text{g/ml}$). The presence of the vectors in the complementary strain was confirmed by PCR.

The complementary plasmid for *recA* gene was derived from pRY107 vector (a gift from Dr. Konkel at Washington State University). The insertion fragment containing upstream (500 bp) and downstream (100 bp) regions of *recA* gene was PCR-amplified using primer pairs of *recA*-CF/*recA*-CR. The amplicon containing *recA* gene was ligated with EcoRI/XbaI-digested pRY107 using NEBuilder® HiFi DNA Assembly Cloning Kit (New England Biolabs® Inc.). The complementary plasmid pRY107-*recA* was transformed into the *C. jejuni* F38011 $\Delta recA$ mutant. Transformants were selected on MH agar supplemented with Kanamycin (20 $\mu\text{g/ml}$). The presence of the vectors in the complementary strain was confirmed by PCR.

Crystal violet biofilm assay

Crystal violet staining assay was applied to quantify the formation level of biofilms developed in 96-well plate (2). After 72-h cultivation, each biofilm in the 96-well plate was washed with sterile deionized water and air dried for 15 min. A total of 200 μl of 0.5% (w/v) crystal violet solution was added into each well of the 96-well plate to stain the biofilm for 15 min. Unbound crystal violet was then washed off using sterile deionized water. Bound crystal violet was dissolved in 200 μl of 95% ethanol (v/v) for 10 min. Signals from the released crystal violet were measured using a microplate reader at 595 nm (SpectraMax M2, Molecular Devices). MH broth without bacterial inoculation was stained using the same method as the control. The control signal was subsequently subtracted for background correction.

Fabrication of microfluidic “lab-on-a-chip” platform for biofilm formation

A polydimethylsiloxane (PDMS)-based microfluidic device was fabricated using soft lithographic technique (3). The schematic image of the fabrication procedure and microfluidic pattern design is described in the supplementary material (**Fig S1**). The in/outlet-connected cultivation chamber was in

the center of the device. The dimensions of inlet and outlet were 400 μm (width) \times 60 μm (height) and the cultivation chamber had a circular shape with a dimension of 300 μm (radius) \times 60 μm (height). The pattern was molded with PDMS and bonded to a glass slide via oxygen plasma treatment. A syringe pump was applied to control the hydrodynamic condition (*e.g.*, flow rate) in the microfluidic device.

Atomic force microscopy

The morphological variation of the biofilm due to DNase I treatment was determined using a Cypher atomic force microscope (Bruker, InnovaTM high-resolution system) with TR400PB tip cantilevers (Bruker, nominal spring constant: $k = 0.02 \text{ N/m}$). *C. jejuni* F38011 biofilm developed on a nitrocellulose membrane was air-dried for 30 min before loading onto the AFM specimen disc (15 mm diameter, Ted Pella) for characterization. Topographic images were collected in the contact mode at 8 random locations on the surface of the biofilm with an area of 8 $\mu\text{m} \times 8 \mu\text{m}$. The scan frequency was maintained at 0.5 Hz. The AFM system was driven using NanoDrive software (Bruker, v8.06) and the AFM images were analyzed off-line using NanoScope software (Bruker, v1.5).

Real-time qPCR analysis of gene expression

The real-time qPCR was performed to plot the expression profile of *flaA* and *flaB* in response to the aerobic and starvation conditions in *C. jejuni* F38011 wild type strain as well as *spoT* and *recA* deletion mutant strains. The total RNA was purified from *C. jejuni* F38011 wild type strain and *spoT* and *recA* deletion mutant strains using RNeasy minikit (Qiagen) according to the manufacturer's protocol. Complementary DNA (cDNA) was reverse transcript using RNA as the template by using SensiFASTTM cDNA Synthesis Kit (Bioline) according to the manufacturer's protocol. The qPCR analysis was performed in triplicate using SensiFAST SYBR Lo-ROX Kit (FroggaBio) on ABI Prism 7000 Fast

instrument (Life Technologies). The *rpoA* gene was used as the internal control. The arbitrary fold change cut-offs was set as more than 2.

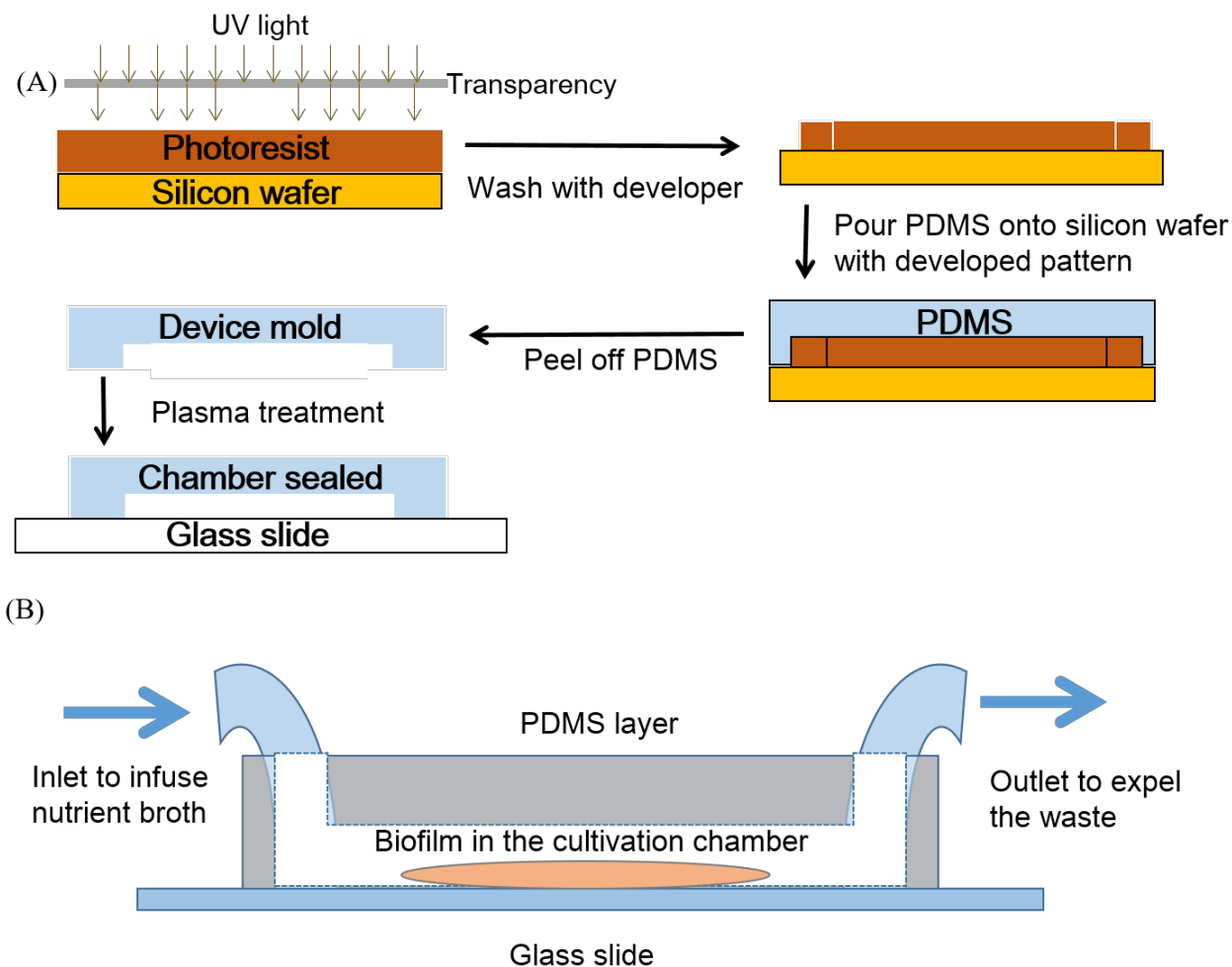


FIG S1. Schematic illustration of the fabrication of microfluidic “lab-on-a-chip” platform. (A) The pattern of microfluidic device was printed on a transparency. A total of 1 mL of SU-3050 permanent epoxy negative photoresist was dispensed on a silicon wafer and spun to achieve a thickness of 60 μm with the following program: 500 rpm for 10 sec with acceleration of 100 rpm/sec and then 3000 rpm for 30 sec with acceleration of 300 rpm/sec. The photoresist on the silicon wafer was then soft baked on a hot plate for 10 min at 95°C. The transparency with a pattern was then loaded on the photoresist for UV exposure. The exposure energy was set as 150 mJ/cm^2 . After UV exposure, the photoresist was baked again at 65°C for 1 min and then 95°C for 5 min. The silicon wafer with photoresist was then washed with SU-8 developer for 10 min to remove the unexposed photoresist. The PDMS was then molded on the

basis of the pattern on the silicon wafer. The inlet and outlet were drilled on PDMS with a puncher before bond onto glass slide using the plasma treatment. (B) The microfluidic platform for biofilm cultivation was consisted of one inlet for the infusion of nutrient broth, one outlet to expel the waste and one cultivation chamber for biofilm cultivation.

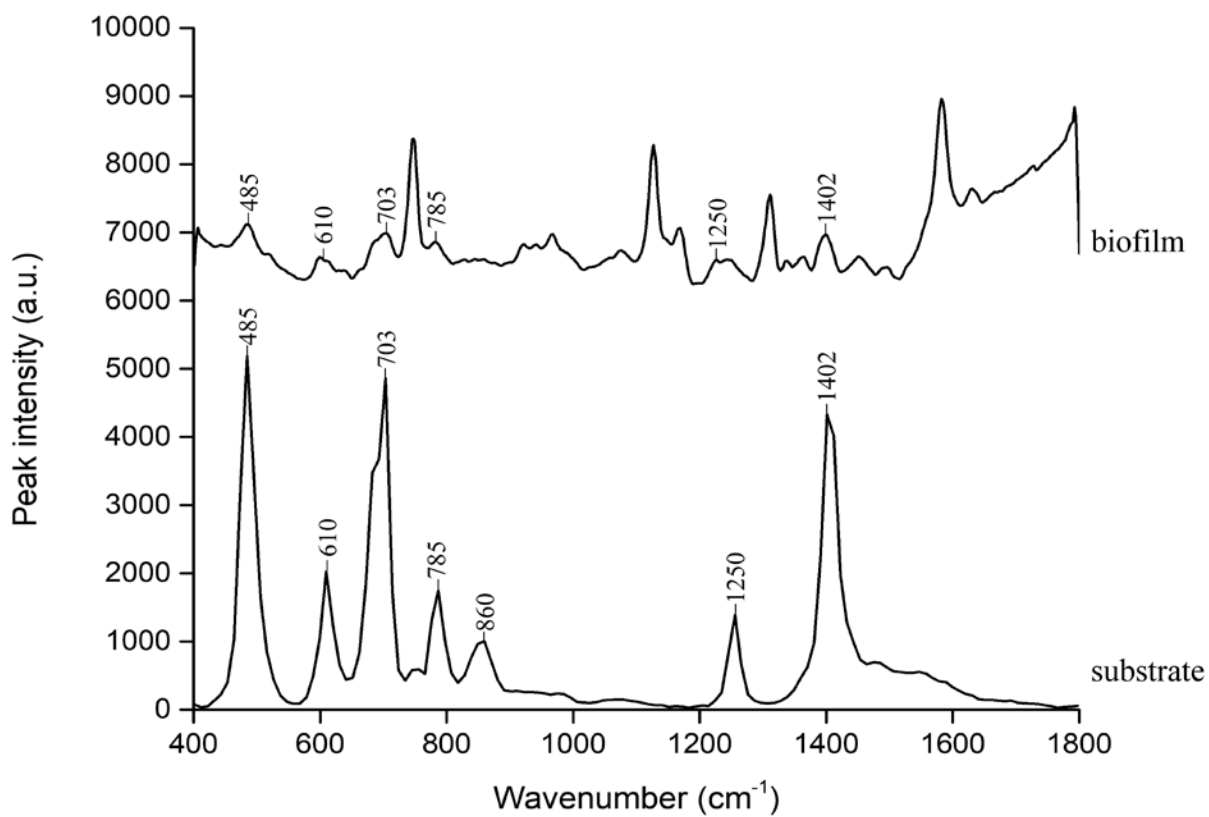


FIG S2. Raman peaks derived from the microfluidic substrate had no overlap with the peaks derived from *C. jejuni* F38011 biofilm. Raman peaks derived from the microfluidic substrate were labeled as highlight.

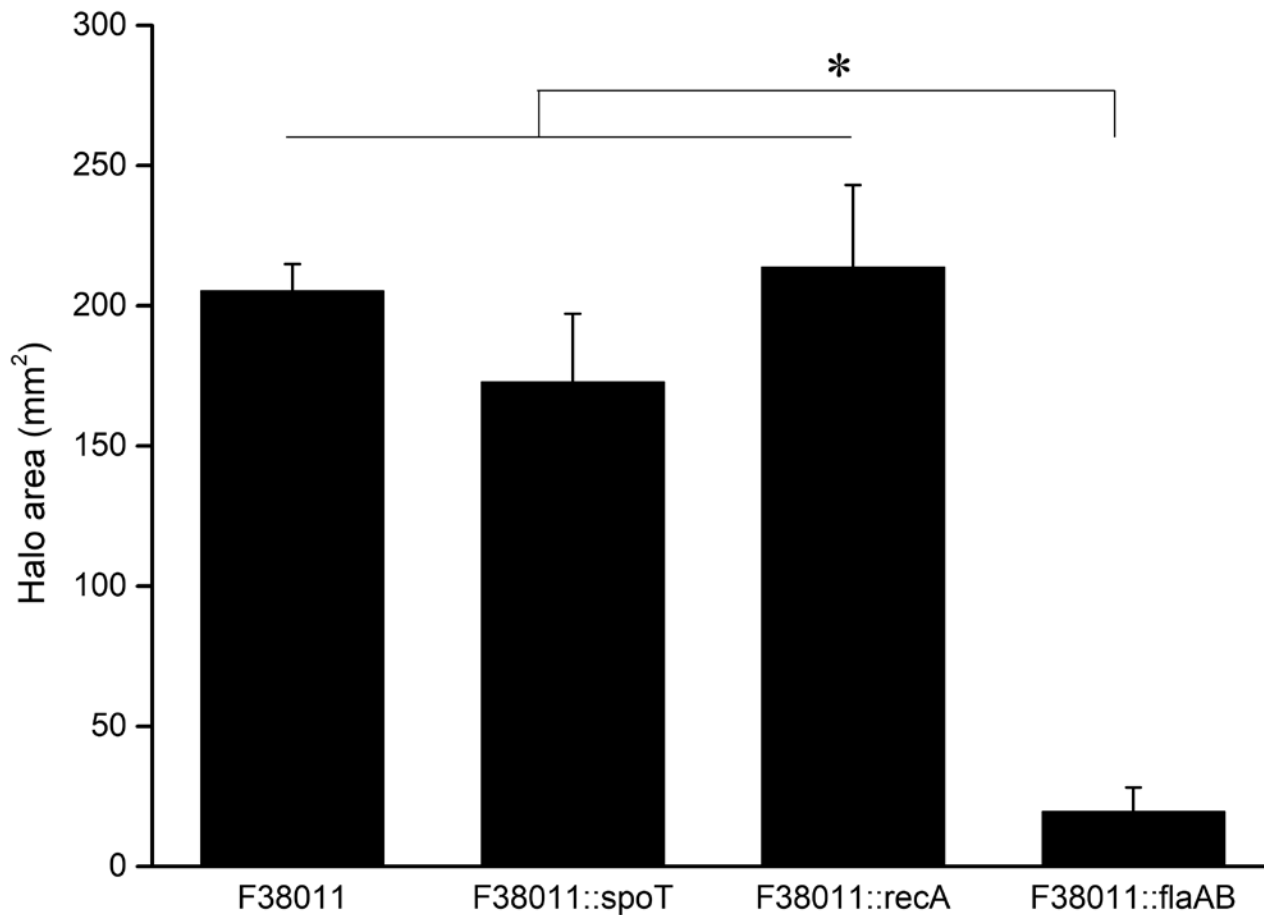


FIG S3. The mutations on *flaA* and *flaB* significantly decreased the motility of *C. jejuni* F38011 while the mutations on *spoT* or *recA* had no influence on the motility of *C. jejuni* F38011. A total of 5 μ l of the overnight bacterial culture was spotted onto the Brucella media supplemented with 0.4% agar. After 2-day cultivation in microaerobic condition at 37°C, the halo area was measured. Asterisk denotes significant difference ($P < 0.05$).

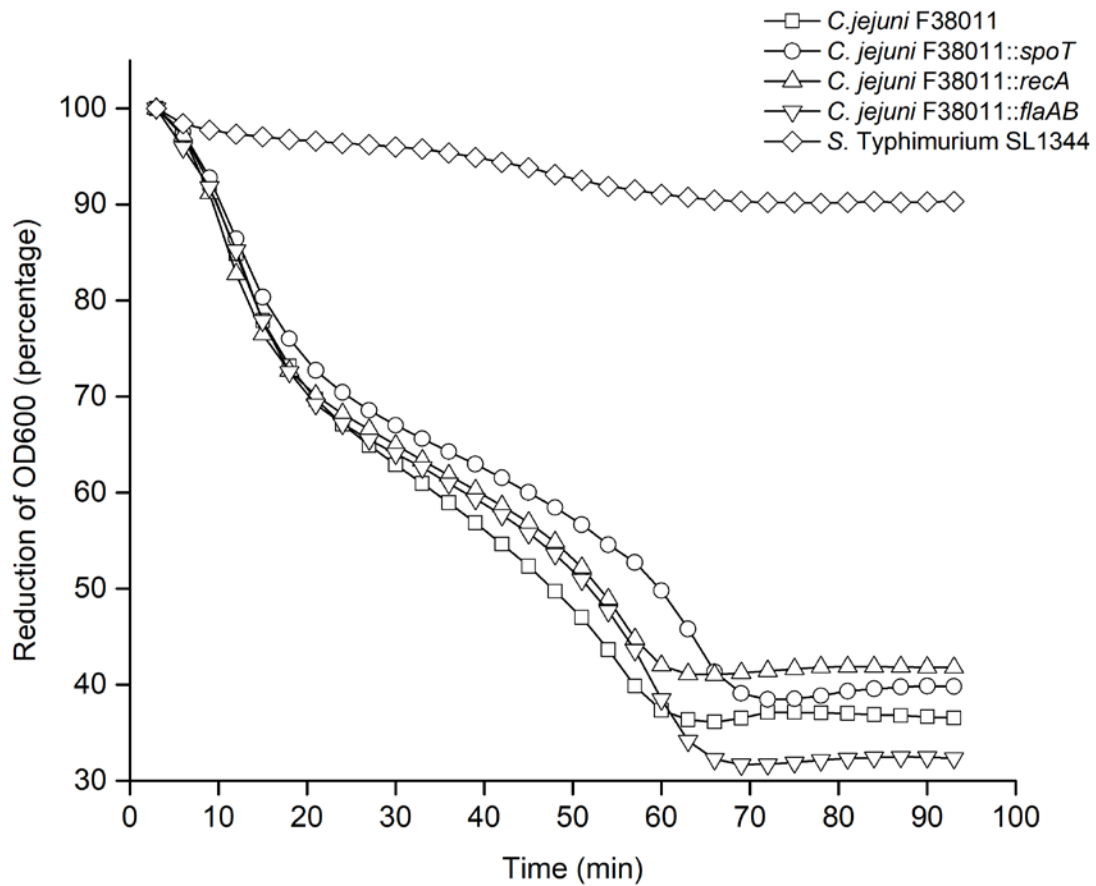


FIG S4. Autolysis level of *C. jejuni* induced by Triton X-100 was significantly higher than that of *S. Typhimurium* SL1344 and autolysis level had no significant difference among *C. jejuni* F38011 wild type, *spoT*, *recA* and *flaAB* deletion mutants. Triton X-100 was dissolved in 0.05 M Tris-HCl to achieve a final concentration of 0.02% (v/v) as the autolysis buffer. Bacterial cells were harvested in the late exponential phase and resuspended in autolysis buffer to 0.3 of OD₆₀₀. The reduction of OD₆₀₀ value was measured every 3 min for a total of 90 min using a microplate reader.

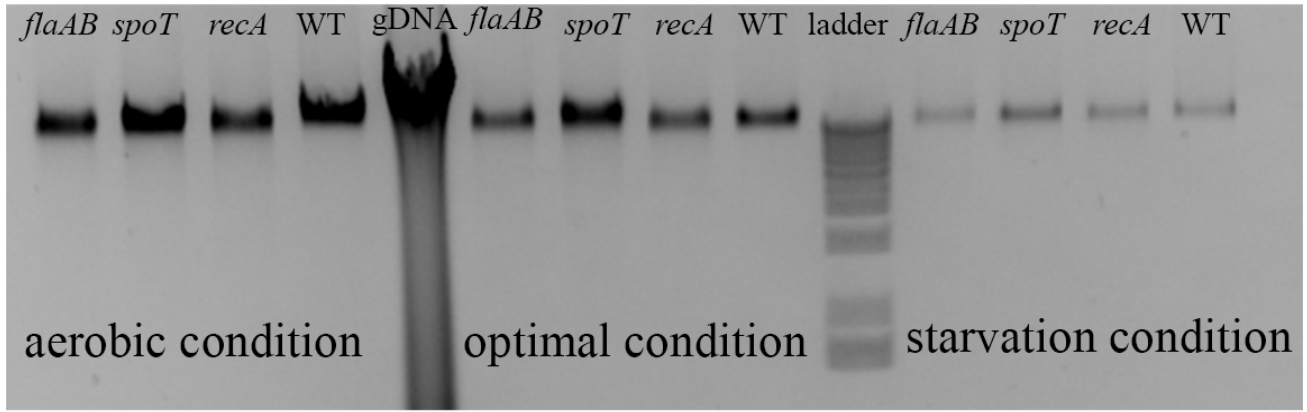


FIG S5. The length of DNA fragment present in *C. jejuni* during biofilm formation was similar to that of genomic DNA extracted from *C. jejuni* F38011 planktonic cells. Gel electrophoresis was performed to demonstrate the length of the released DNA fragment. After 3-day biofilm cultivation, each bacterial culture in the 96-well plate was collected. A total of 10 μ l of the supernatant was mixed with 2 μ l of DNA loading dye solution and then loaded in 1% agarose gel for electrophoresis. A 1-kb ladder was used as the reference. The DNA was stained using SYBRTM safe DNA gel stain and visualized on ChemiDocTM XRS gel documentation system.

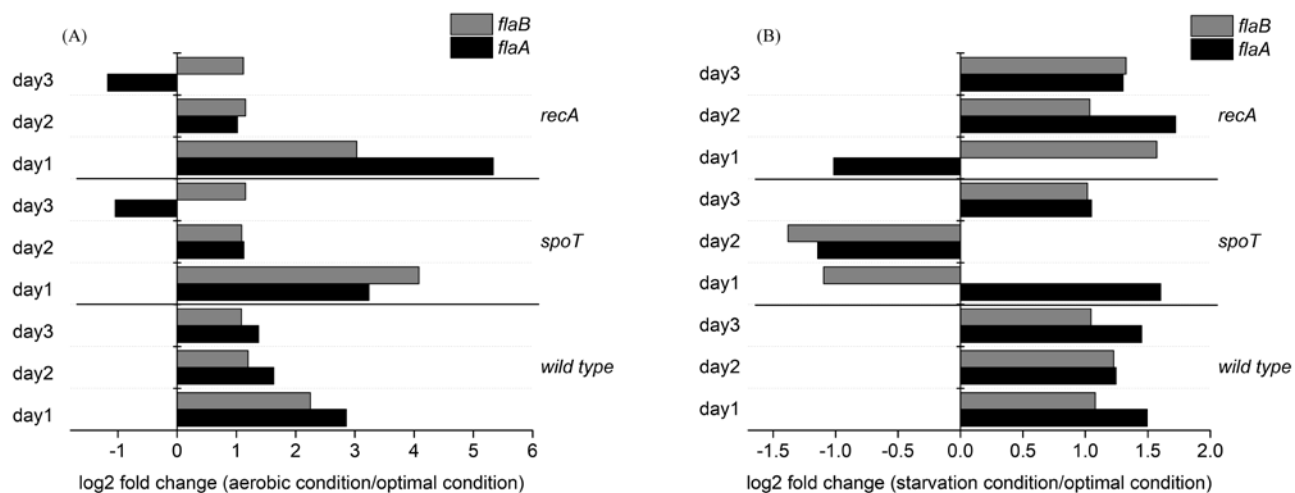


FIG S6. Expression of *flaA* and *flaB* genes in *C. jejuni* F38011 wild type, *spoT* and *recA* deletion mutants was upregulated only at the first day of biofilm formation under aerobic condition. Real-time qPCR was performed to plot the expression profile of *flaA* and *flaB* in response to the aerobic condition (A) and starvation condition (B) in *C. jejuni* F38011 wild type strain as well as *spoT* and *recA* deletion mutant strains. The *rpoA* gene was used as the internal control. The arbitrary fold change cut-offs was set as more than 2.

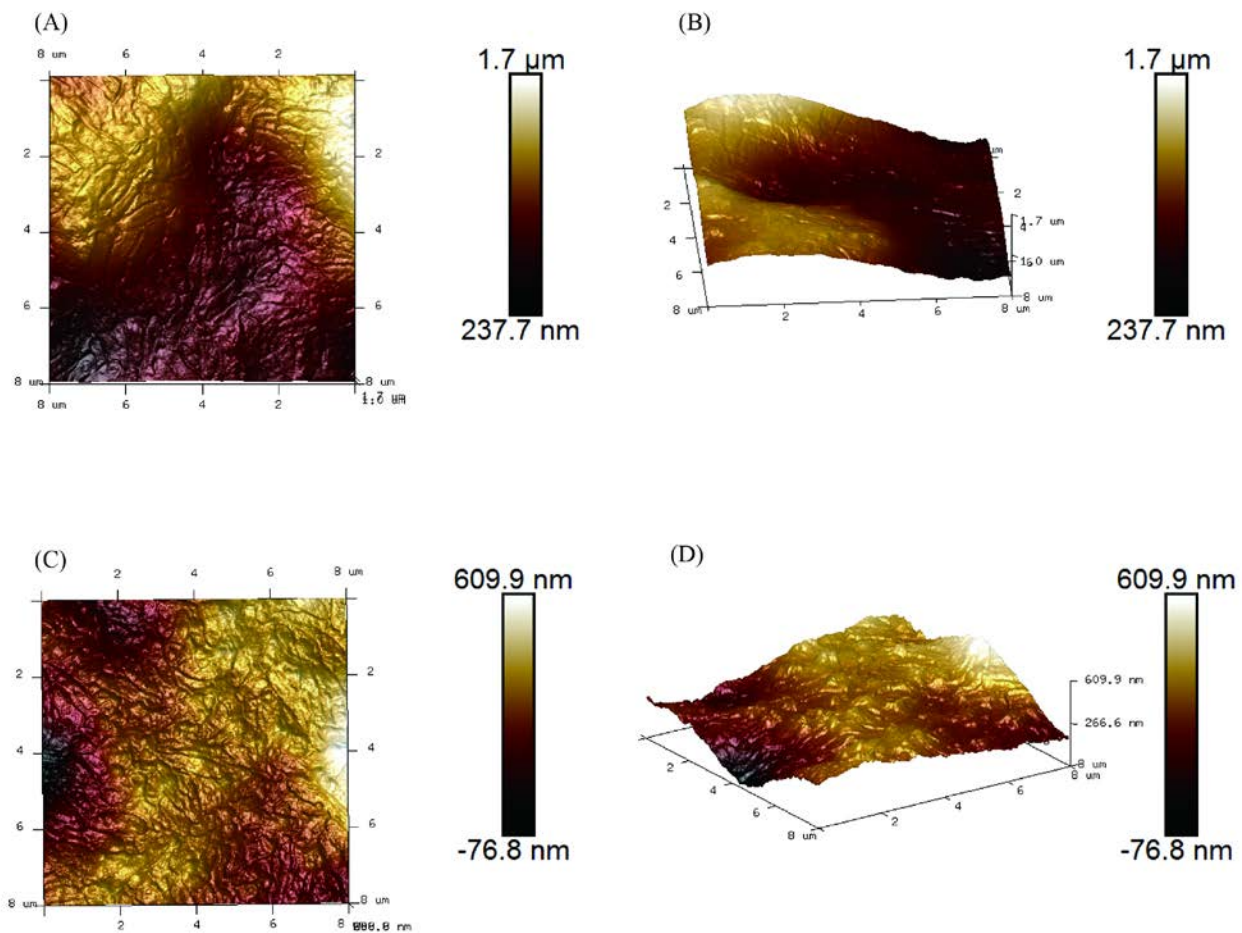


FIG S7. Topographic images of *C. jejuni* F38011 biofilms confirmed that the DNase I treatment disrupted biofilm structure and dispersed encased *C. jejuni* F38011 cells. The images were obtained by atomic force microscopy in contact mode within $8\ \mu\text{m} \times 8\ \mu\text{m}$ area at scan frequency of 0.5 Hz: (A) *C. jejuni* biofilm without DNase I treatment; (B) 3D reconstruction of the untreated *C. jejuni* biofilm; (C) *C. jejuni* biofilm after DNase I treatment ; (D) 3D reconstruction of the treated *C. jejuni* biofilm.

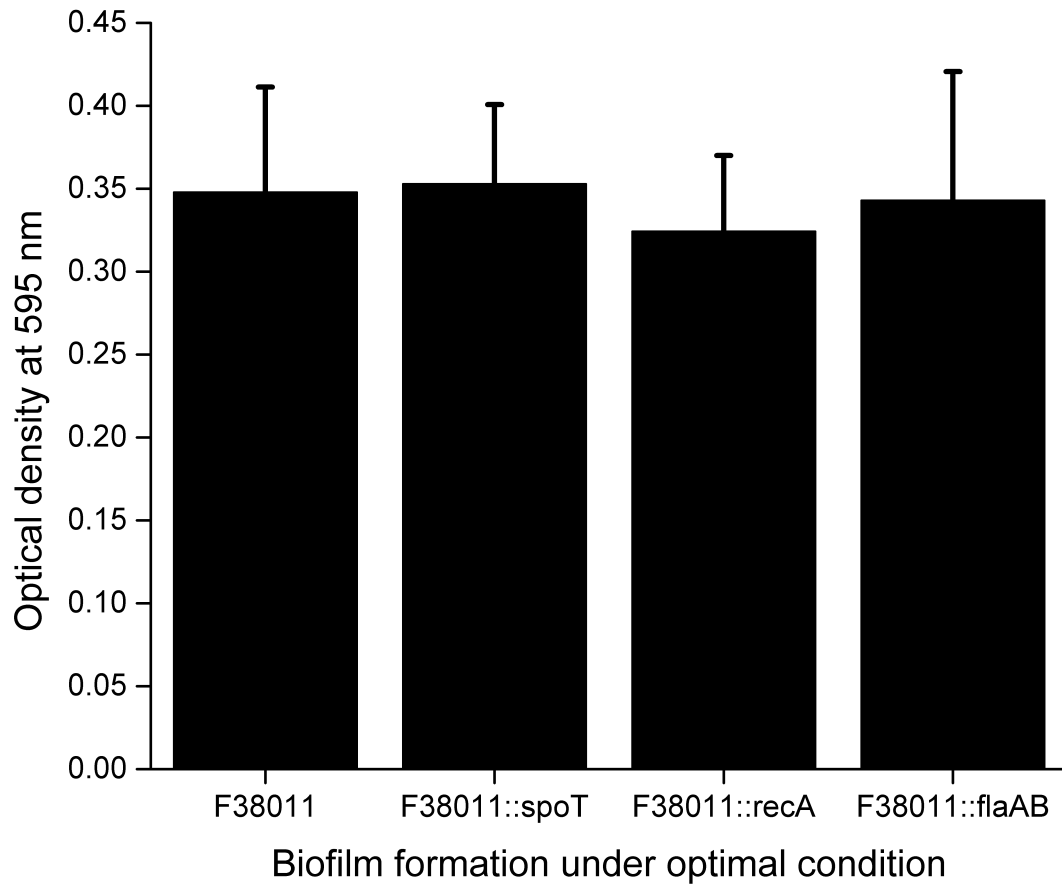


FIG S8. Biofilm formation of *C. jejuni* F38011 complementary strains including *spoT*, *recA* and *flaAB* under optimal condition.

TABLE S1. Bacterial strains and plasmid used in the current study.

| Strain or plasmid | Description | Reference |
|-----------------------------------------------|-----------------------------------------------------------------------------------------------------------------------------------|--------------------------------------------------------------------------------------|
| Strains | | |
| <i>C. jejuni</i> F38011 | human clinical isolate | (4) |
| <i>C. jejuni</i> Human 10 | human clinical isolate | (5) |
| <i>C. jejuni</i> 81116 | human clinical isolate | (6) |
| <i>C. jejuni</i> ATCC 33560 | product, quality control strain | ATCC company |
| <i>C. jejuni</i> 87-95 | human clinical isolate | Laboratory collection obtained from Dr. Michael Konkel (Washington State University) |
| <i>C. jejuni</i> NCTC 11168 | human clinical isolate | (7) |
| <i>C. jejuni</i> 1658 | environmental isolate | Laboratory collection obtained from Dr. Götz, Greta (Free University Berlin) |
| <i>C. jejuni</i> F38011 Δ <i>spoT</i> | <i>spoT</i> gene deletion mutant of <i>C. jejuni</i> F38011 strain, Kan ^R | This study |
| <i>C. jejuni</i> F38011 Δ <i>recA</i> | <i>recA</i> gene deletion mutant of <i>C. jejuni</i> F38011 strain, Cm ^R | This study |
| <i>C. jejuni</i> F38011 Δ <i>flaAB</i> | <i>flaA</i> and <i>flaB</i> genes deletion mutant of <i>C. jejuni</i> F38011 strain, mobility deficiency mutant, Tet ^R | (6) |
| <i>C. jejuni</i> F38011:: <i>spoT</i> | <i>spoT</i> gene complementary strain | This study |

| | | |
|----------------------------------------|----------------------------------------------------------------------------------------------|-------------------------------------------------------------------|
| | of <i>C. jejuni</i> F38011, Kan ^R &Cm ^R | |
| <i>C. jejuni</i> F38011:: <i>recA</i> | <i>recA</i> gene complementary strain | This study |
| | of <i>C. jejuni</i> F38011, Cm ^R &Kan ^R | |
| <i>C. jejuni</i> F38011:: <i>flaAB</i> | <i>flaA</i> and <i>flaB</i> genes | (6) |
| | complementary strain of <i>C. jejuni</i> F38011, Tet ^R &Cm ^R | |
| <i>C. jejuni</i> GFP | green fluorescent protein | (8) |
| | expression strain of <i>C. jejuni</i> F38011, Kan ^R | |
| <i>S. Typhimurium</i> SL1344 | Human clinical isolate | (9) |
| <i>S. Typhimurium</i> SL1344 - RFP | Red fluorescent protein expression of <i>S. Typhimurium</i> SL 1344 strain, Str ^R | (9) |
| <i>E. coli</i> DH5α | product, generation of recombinant plasmids | Invitrogen |
| Plasmid | | |
| pUC19 | product, suicide vector, Amp ^R | Invitrogen |
| pUC18K2 | cloning vector, Kan ^R | (10) |
| pRY111 | cloning vector, Cm ^R | (11) A gift from Dr. Michael Konkel (Washington State University) |
| pRY107 | cloning vector, Kan ^R | A gift from Dr. Michael Konkel (Washington State University) |

Cm^R strands for chloramphenicol resistance (8 µg/ml); Amp^R strands for ampicillin resistance (100

$\mu\text{g/ml}$); Kan^R strands for kanamycin resistance (50 $\mu\text{g/ml}$); Str^R strands for streptomycin resistance (100 $\mu\text{g/ml}$). Tet^R strands for tetracycline resistance (10 $\mu\text{g/ml}$)

TABLE S2. Primers used in the current study.

| Primer | Sequence (5'-3') |
|-----------------|--------------------------------------------------------------|
| <i>spoT</i> -FF | CGGAATTCAAGTGGAGAGCCTTATGCGG |
| <i>spoT</i> -FR | CTTGGTACCGTCTATGGGCTATTGGGGCA |
| <i>spoT</i> -RF | GCGGATCCAGCCAGACGTATTAGACAAGTA GC |
| <i>spoT</i> -RR | GATCTAGATCTCAAATAATCTACCGCCGA |
| <i>kan</i> -F | TGTATATGCCCAATAGCCGGTACCCGGGT GACTAACTAGGAGGAATAA |
| <i>kan</i> -R | GCTACTTGTCTAATACGTCTGACGGATCCCC GGGTCATTATTCCCTCCAGGTA |
| <i>recA</i> -FF | TTGTAAAACGACGGCCAGTGATTCAACGCC TTTTCCGCCAAATC |
| <i>recA</i> -FR | AGCAACGCGATCTAGCTATCGCGGCCTAGG GTACC GGAGAGGGTTTAAGCCGTGA |
| <i>recA</i> -RF | ATATTAGTTCGATTCAACAT GGATCCACATCAAGCGCATGTTCTGC |
| <i>recA</i> -RR | CAAGCTTGCATGCCTGCAGGTCGACTCTAG ATGCTGTGCGTAAAAGTGCAT |
| <i>cm</i> -F | TCACGGCTTAAACCCTCTCCGGTACCTTACG CCCCGCCCTGCCATCATCGCAGTA |
| <i>cm</i> -R | GCAGAACATGCGCTTGATGTGGATCCATCG |

| | |
|-----------------|--------------------------------|
| | AGATTTTCAGGAGCTAAGGAAGCTAA |
| <i>flaA</i> -F | GCTTATGCTATAAAAAGCAGGTTCA |
| <i>flaA</i> -R | GTCAACCTTACCTATAGTCACACCA |
| <i>flaB</i> -F | AACAGGAGTTCGTGCAACTT |
| <i>flaB</i> -R | CATCCGATGTTTTTCCAGACTTTA |
| <i>rpoA</i> -F | CGAGCTTGCTTTGATGAGTG |
| <i>rpoA</i> -R | AGTTCCACAGGAAAACCTA |
| <i>spoT</i> -CF | CGGTATCGATAAGCTTGATATCGAATTCGC |
| | GCTGTAGGATCAAACCCT |
| <i>spoT</i> -CR | GCTCCACCGCGGTGGCGGCCGCTCTAGAAG |
| | AGCTGTGGAAATTGATGCAG |
| <i>recA</i> -CF | CGGTATCGATAGGCTTGATATCGAATTCAC |
| | CACTTGGA ACTATGGCCG |
| <i>recA</i> -CR | GCTCCACCGCGGTGGCGGCCGCTCTAGATT |
| | GCTCCACTCAAAGCGACT |

TABLE S3. Raman band assignments for *C. jejuni* biofilm formed in the microfluidic platform (12-14).

| Raman shift (cm ⁻¹) | Band assignment |
|---------------------------------|-----------------------------------------------------------------------------|
| 746 | T ring breathing mode of DNA/RNA base |
| 918 | amino acid, proline ring |
| 968 | lipid representative band |
| 1125 | skeletal of acyl backbone in lipid and C-N stretching in protein vibration |
| 1168 | lipids $\nu(\text{C}=\text{C})$ $\nu(\text{COH})$ |
| 1310 | CH ₃ /CH ₂ twisting or bending mode of lipid/collagen |
| 1370 | saccharide representative band |
| 1453 | umbrella mode of methoxyl in protein |
| 1580 | pyrimidine ring in nucleic acids |

VIDEO S1. In *C. jejuni*-*Salmonella* dual-species biofilm, *Salmonella* cells did not interact directly with eDNA but instead distributed around eDNA-rich structures. *Salmonella* cells are red, eDNA is blue, and *C. jejuni* cells are green.

References

1. Davis L, Young K, DiRita V. 2008. Genetic manipulation of *Campylobacter jejuni*. *Curr Protoc Microbiol*:8A. 2.1-8A. 2.17.
2. Feng J, De La Fuente-Núñez C, Trimble MJ, Xu J, Hancock RE, Lu X. 2015. An *in situ* Raman spectroscopy-based microfluidic “lab-on-a-chip” platform for non-destructive and continuous characterization of *Pseudomonas aeruginosa* biofilms. *Chem Commun* 51:8966-8969.
3. Qin D, Xia Y, Whitesides GM. 2010. Soft lithography for micro-and nanoscale patterning. *Nat Protoc* 5:491.
4. Feng J, Lamour G, Xue R, Mirvakliki MN, Hatzikiriakos SG, Xu J, Li H, Wang S, Lu X. 2016. Chemical, physical and morphological properties of bacterial biofilms affect survival of encased *Campylobacter jejuni* F38011 under aerobic stress. *Int J Food Microbiol* 238:172-182.
5. Li J, Feng J, Ma L, de la Fuente Núñez C, Götz G, Lu X. 2017. Effects of meat juice on biofilm formation of *Campylobacter* and *Salmonella*. *Int J Food Microbiol* 253:20-28.
6. Neal-McKinney JM, Christensen JE, Konkel ME. 2010. Amino-terminal residues dictate the export efficiency of the *Campylobacter jejuni* filament proteins via the flagellum. *Mol Microbiol* 76:918-931.
7. Parkhill J, Wren B, Mungall K, Ketley J. 2000. The genome sequence of the food-borne pathogen *Campylobacter jejuni* reveals hypervariable sequences. *Nature* 403:665.
8. Mixter PF, Klena JD, Flom GA, Siegesmund AM, Konkel ME. 2003. In vivo tracking of *Campylobacter jejuni* by using a novel recombinant expressing green fluorescent protein. *Appl Environmental Microbiol* 69:2864-2874.
9. Knodler LA, Vallance BA, Celli J, Winfree S, Hansen B, Montero M, Steele-Mortimer O. 2010. Dissemination of invasive *Salmonella* via bacterial-induced extrusion of mucosal epithelia. *Proc*

Natl Acad Sci USA 107:17733-17738.

10. Gaynor EC, Wells DH, MacKichan JK, Falkow S. 2005. The *Campylobacter jejuni* stringent response controls specific stress survival and virulence-associated phenotypes. *Mol Microbiol* 56:8-27.
11. Buelow DR, Christensen JE, Neal-McKinney JM, Konkel ME. 2011. *Campylobacter jejuni* survival within human epithelial cells is enhanced by the secreted protein CiaI. *Mol Microbiol* 80:1296-1312.
12. Movasaghi Z, Rehman S, Rehman IU. 2007. Raman spectroscopy of biological tissues. *Appl Spectrosc Rev* 42:493-541.
13. Talari ACS, Movasaghi Z, Rehman S, Rehman IU. 2015. Raman spectroscopy of biological tissues. *Appl Spectrosc Rev* 50:46-111.
14. Naumann D. 2001. FT-infrared and FT-Raman spectroscopy in biomedical research. *Appl Spectrosc Rev* 36:239-298.